An internal-integrated RED/ED system for energy-saving seawater desalination: A model study

Man Chen[a]*, Ying Mei[b], Yuqing Yu[a], Raymond Jianxiong Zeng[a], Fang Zhang[a], Shungui Zhou[a], Chuyang Y. Tang[b]

[a]Fujian Provincial Key Laboratory of Soil Environmental Health and Regulation, College of Resources and Environment, Fujian Agriculture and Forestry University, Fuzhou 350002, China

[b]Department of Civil Engineering, The University of Hong Kong, Pokfulam, Hong Kong 999077

[*]**Corresponding author**.

Fujian Provincial Key Laboratory of Soil Environmental Health and Regulation, College of Resources and Environment, Fujian Agriculture and Forestry University, Fuzhou 350002, China

Email address: chenman@fafu.edu.cn (Dr. Man Chen)

Abstract:

Salinity gradient energy extracting by a reverse electrodialysis (RED) unit using for electrodialysis (ED) desalination process is a potential way to achieve energy-economic and sustainable production of freshwater. However, the parameters in RED and ED unit synergistically influence the desalination process, resulting to the hybrid process controlled by multi-parameters. Modeling of an RED/ED is a simple way to describe the desalination process and reveal the effects of these parameters on the performance of system and then to find the better adaption of RED/ED. In this study, a model of an internal-integrated RED/ED hybrid system is first established. It found that the ratio of desalination in RED/ED is higher than 90%. The brine/river is the alternative combination to realize seawater desalination with a desalination rate of 0.38 h•m^2/mol. The desalination capacity of RED/ED (0.43-2.6 mol/h•m^2) is much higher than that of the external-integrated RED+ED system (0.10-0.15 mol/h•m^2), but it is of simpler configuration and has a lower energy requirement. Moreover, the RED/ED system is preferred for using in the pre-desalination process. The outcome of this model is helpful in the design of practical RED/ED systems, and points out the development potential of RED/ED in practical applications.

Keywords: desalination; electrodialysis; reverse electrodialysis; hybrid system; modeling

1. Introduction

Desalination of seawater has become the most attractive way to solve freshwater scarcity [1]. Generally, desalination technologies include membrane-based (reverse osmosis or electrodialysis) and thermal distillation-based (multieffect distillation, multistage flash, or vapor compression) desalination processes [2, 3]. Among them, electrodialysis (ED) has high water recovery and low maintenance costs, being a potential alternative for desalination, especially in water-stressed remote locations [4]. However, the energy consumption of ED, in the range of 0.7~5.5 kwh/m^3, is higher than that of other membrane based desalination processes, like reverse osmosis [5, 6]. To find an economic ED process, renewable energy (wind or solar energy) is often used to drive the ED process [4, 7]. However, expensive capital energy conversion systems and complicated technology designs make hybrid systems difficult to apply [5]. For example, in a solar/ED process, a photovoltaic solar panel, charge regulator, storage batteries, *etc.*, are required to first transform solar energy into electricity, then drive ED desalination [5]. Therefore, a simply hybrid system that utilizes renewable energy in the ED process is of great importance for economic desalination.

Reverse electrodialysis (RED) is the inverse process of ED [8-10]. It can draw electrical energy from salinity gradient energy between two streams at different concentrations [9, 11]. The configuration of an RED device is similar to that of an ED device, consisting an electrode system, alternately stacking ion exchange membranes (IEMs) and two streams [12]. Therefore, the RED device and the ED device can be easily coupled in one module without any other special connection. Meanwhile, RED is an excellent method for brine management, in which the brine generated from ED is capable of acting as the high-salinity stream of RED and can then be adequately diluted to assist in its environmental discharge [13, 14]. Additionally, energy extracted

from RED can be utilized to offset the energy consumption of ED to achieve low-energy desalination [15]. The theoretical energy extracted by RED is in the range of 0.22 -14 kwh/m^3, which is enough to drive an ED for desalination (0.7~5.5 kwh/m^3) [10]. Therefore, coupling RED with ED will realize economic desalination in an easy operation mode meanwhile with good brine management.

Recently, a RED+ED hybrid system in an external-integrated form was proposed, in which high-salt wastewater first flowed across the standalone RED unit for pre-desalting and was then guided into the ED unit for deep desalination, which would cost large amount of energy (17.5~20.1 kWh/m^3) [15]. Although a power-free ED for desalination is feasible in RED+ED, a large amount of gradient difference energy from RED is consumed in the conversion of chemical energy to electrical energy and then to chemical energy again, resulting to a low energy efficiency [16]. By contrast, a RED/ED hybrid unit in an internal-integrated form, in which the desalination process is directly driven by the ion current, would reduce energy waste in the process of energy conversion. Moreover, only one electrode (note: Pt/Ti as the electrode) is required in RED/ED, while two couples of electrodes are used in the external-integrated form. It has been proven to be energy self-sufficient to produce drinkable water through RED/ED [17]. However, the performance of internal-integrated RED/ED devices is affected by many factors, such as the concentration of each stream, the numbers of stacks, the thickness of channels, etc. As a multi-parameter control process, modeling of RED/ED is a simple way to explore the effects of these parameters on the performance of system and then to find the better adaption of RED/ED. Although extensive models of RED or ED were constructed previously, the model of RED/ED coupling is still required because the parameters of RED and ED synergistically affect the process of desalination. For

example, both of the stacking numbers and concentration of streams of RED or ED contribute to the resistance and electromotive force. Besides, the resistance and electromotive force of system changes with desalination process. Until now, few studies have systematically investigated the effects of these factors on the RED/ED desalination process. Therefore, a systematic investigation of RED/ED is necessary and meaningful to reveal the future of RED/ED.

In this study, a mathematical model of an internal-integrated RED/ED device was established. Through modeling of the RED/ED hybrid system, the basic requirements, the desalination process and the design parameters of the RED/ED system were investigated to identify the better method of integration in a practical RED/ED system. The capacity for desalination and the energy consumption of internal-integrated RED/ED, external-integrated RED+ED, standalone ED, solar/ED and wind/ED systems were compared. It is anticipated that this model might be helpful in the design of RED/ED systems, and might show the development potential of RED/ED for practical application.

2. Process description and model development

2.1 Modeling of ED unit operations

A simplified scheme of the ED system is shown in **Figure 1a**. A conventional ED device mainly contains four parts: a direct current supply, two electrodes, alternately stacked IEMs and feed/permeate solutions [18]. The feed and permeate solutions are alternately separated by a cation exchange membrane (CEM) and an anion exchange membrane (AEM). When an electric field is applied to the electrodes, cations transport through th CEM to th cathode, while anions transport through the AEM to the anode. This causes a decreasing concentration of the feed solution and an increasing concentration of the permeate solution. Therefore, the potential difference

($\Psi_{ED,q}$) between the permeate solution and feed solution gradually increases with the desalination ratio q. q is defined in **Eq. (1)**.

$$q = \frac{C_{f,q}}{C_{f,0}} \quad (1 \geq q \geq 0) \tag{1}$$

in which $C_{f,q}$ is the concentration of the feed solution when the desalination ratio is equal to q. $C_{f,0}$ is the initial concentration of the feed solution.

$\Psi_{ED,q}$ is calculated based on the Nernst Equation [19]:

$$\Psi_{ED,q} = \frac{N_{ED}RT}{F}\left(\frac{\alpha_{CEM}}{z^{+}} + \frac{\alpha_{AEM}}{z^{-}}\right)\ln\left(\frac{\gamma_{\pm,p}C_{p,q}}{\gamma_{\pm,f}C_{f,q}}\right) \tag{2}$$

in which N_{ED} is the number of membrane pairs in the ED stack, α_{AEM} and α_{CEM} are the permselectivities of AEM and CEM, respectively, R is the gas constant, T is the absolute temperature (K), F is the Faraday constant, z is the valence of the ions, C is the concentration of solution, $\gamma_{\pm}$ is the mean activity coefficient of the solution, the subscripts p and f are refer to the permeate solution and feed solution, respective, and the superscripts + and –refer to cations and anions, respectively. $C_{p,q}$ is the concentration of the feed solution when the desalination ratio is equal to q.

As the concentrations of the feed solution and permeate solution change in the desalination process, the resistance of ED ($R_{ED,q}$) also varies with q [20]:

$$R_{ED,q} = \frac{N_{ED}}{A_m}\left(\overline{R}_{AEM} + \overline{R}_{CEM} + \frac{\delta}{f_v \Lambda_{m,p} C_{p,q}} + \frac{\delta}{f_v \Lambda_{m,f} C_{f,q}}\right) \tag{3}$$

in which A_m is the area of each membrane, δ denotes the thickness of the fluid channels and Λ_m is the equivalent conductivity of the solution. $\overline{R}_{AEM}$ and $\overline{R}_{CEM}$ are the area resistance values for the AEM and CEM, respectively. f_v is called the obstruction factor and represents a correction term for the solution resistance caused by the presence of spacers [21].

When applying a direct current in ED, the rate of ion transfer in the feed solution

is proportional to the current applied [19, 22]:

$$-\frac{\mathrm{d}}{\mathrm{dt}}(C_{f,q}V_f) = \eta\frac{N_{ED}I}{zF} \tag{4}$$

in which V_f is the volume of the feed solution, I is the current of the circuit, and η is the current efficiency. The current efficiency η is the ratio of the amount of ion transferred to the total charge supplied. The ratio depends on the properties of the membranes and solutions.

2.2 Modeling of RED unit operations

Figure 1b shows the simplified scheme of RED. The configuration of an RED device is similar to that of the ED device, but a direct current supply is not included in the former. When concentrated and dilute solutions flux into two adjacent channels separated by an IEM, the chemical potential difference between the solutions will drive cations to diffuse through the CEM and anions to diffuse through the AEM. When connecting the electrode system, the chemical potential is converted into electric potential (E_{RED}), which is calculated based on the Nernst Equation [8]:

$$E_{RED} = \frac{N_{RED}RT}{F}\left(\frac{\alpha_{AEM}}{z^-} + \frac{\alpha_{CEM}}{z^+}\right)\ln\left(\frac{C_h}{C_l}\right) \tag{5}$$

in which N_{RED} is the number of membrane pairs in the RED stack, the subscripts h and l refer to high- and low- salinity water in RED part, C_h and C_l are the concentrations of the high-salinity water and low-salinity water, respectively.

Assuming an RED in a continuous mode, the concentrations in the water compartments are constant. The resistance of RED part (R_{RED}) can be expressed as follow [23]:

$$R_{RED} = \frac{N_{RED}}{A_m}\left(\overline{R}_{AEM} + \overline{R}_{CEM} + \frac{\delta}{f_v \Lambda_m C_h} + \frac{\delta}{f_v \Lambda_m C_l}\right) \tag{6}$$

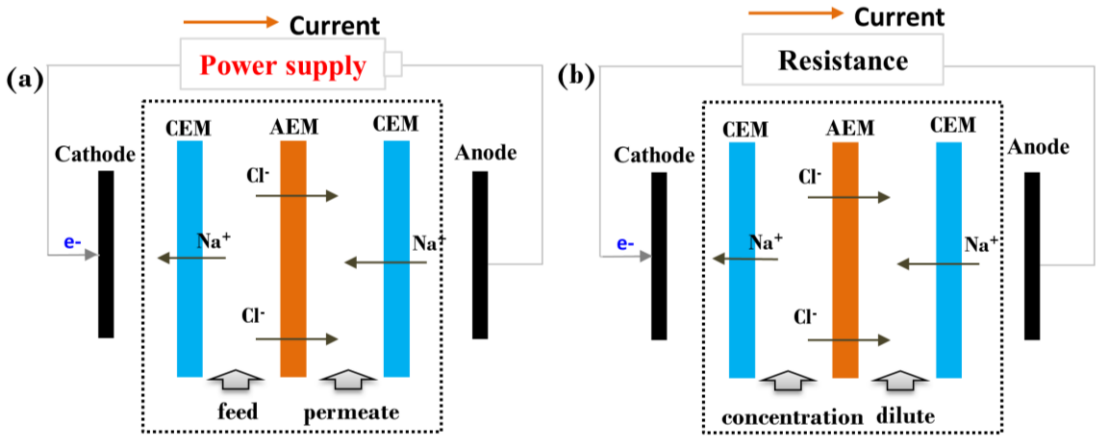

Figure 1 Simplified schemes of ED unit (**a**) and RED unit (**b**).

2.3 Modeling of the internal-integrated RED/ED hybrid system

In an internal-integrated RED/ED hybrid system (**Figure 2**), the salinity gradient energy of the high-salinity solution and low-salinity solution is harvested by the RED and is then used to overcome the energy requirement of ion movement across the membranes in the ED unit. For spontaneous desalination, the salinity gradient energy of RED must be higher than that of ED. Therefore, the theoretical requirements of a RED/ED device working should fulfill the following expression:

$$E_{RED} > \Psi_{ED,q} \tag{7}$$

The total resistance of the RED/ED hybrid system ($R_{tot,q}$) is the sum of the resistance of the RED unit and that of the ED unit. $R_{tot,q}$ also changes with the desalination process:

$$R_{tot,q} = R_{RED} + R_{ED,q} \tag{8}$$

Substituting **Eqs. (6)**, **(9)** to **(11)**, it is found that:

$$R_{tot,q} = \frac{(\overline{R}_{AEM} + \overline{R}_{CEM})}{A_m}(N_{RED} + N_{ED}) + \frac{\delta}{f_v \Lambda_m A_m}\left(\frac{N_{ED}}{C_{p,q}} + \frac{N_{ED}}{C_{f,q}} + \frac{N_{RED}}{C_h} + \frac{N_{RED}}{C_l}\right) \tag{9}$$

An area resistance $\frac{R_{tot,q}}{(N_{ED} / A_m)}$ ($\Omega \cdot m^2$) is used to normalize the desalination capacity and the value does not depend on the stacking numbers of cells or the area of

each membrane in the ED unit.

$$\frac{R_{tot,q}}{(N_{ED}/A_m)} = (\overline{R}_{AEM} + \overline{R}_{CEM})(\frac{N_{RED}}{N_{ED}} + 1) + \frac{\delta}{\Lambda_m f_v}(\frac{1}{C_{p,q}} + \frac{1}{C_{f,q}} + \frac{\frac{N_{RED}}{N_{ED}}}{C_h} + \frac{\frac{N_{RED}}{N_{ED}}}{C_l}) \quad (10)$$

The current density (i) of the RED-ED hybrid system is calculated based on Ohm's law,

$$i = \frac{E_{RED} - \Psi_{ED}}{A_m R_{tot,q}} \quad (11)$$

The rate of ion transfer in the feed solution is expressed as follows:

$$-\frac{\mathrm{d}}{\mathrm{d}t}(C_{f,q}V_f) = \eta\frac{N_{ED}(E_{RED} - \Psi_{ED})}{zFR_{tot,q}} \quad (12)$$

As it is assumed that the electro-osmotic flux is neglected during the desalination process in ED, the volume of the feed solution is unchanged during the desalination process. Therefore, **Eq. (12)** is also expressed as follows:

$$-\frac{V_f zF}{\eta N_{ED}}\frac{R_{tot,q}}{(E_{RED} - \Psi_{ED,q})}\mathrm{d}C_{f,q} = dt \quad (13)$$

The normalized time ($k = t\frac{(N_{ED}A_m)}{(C_{f,0}V_f)}$, h•m^2/mol) normalizes the molar mass of the feed solution ($C_{f,0}V_f$) and the effective desalination membrane area ($N_{ED}A_m$) in the ED unit.

For the spontaneity of RED driving ED, the required energy is mainly used for pumping. Both the RED and ED systems involve power consumption for pumping as an internal loss [16]. The pump power (P_{pump}, W/m^2) is expressed as a function of the pressure drop, the flow rate and the area of the membrane and is estimated as follows [24]:

$$P_{pump} = \frac{\Delta p_h Q_h + \Delta p_l Q_l}{N_{RED} A_m} + \frac{\Delta p_f Q_f + \Delta p_p Q_p}{N_{ED} A_m} \quad (14)$$

where Δp_h, Δp_l, Δp_f, and Δp_p are the pressure drops along the high-salinity solution compartment, low-salinity solution compartment, feed solution compartment and permeate solution compartment, respectively. Q_h, Q_l, Q_f and Q_p are the volumetric flow rates of the corresponding compartments.

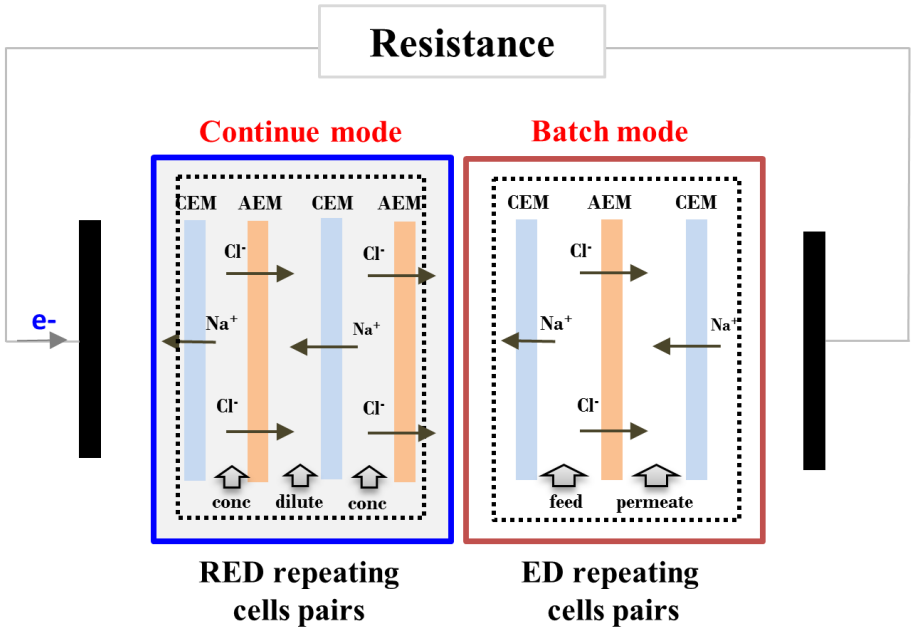

Figure 2 Simplified scheme of the internal-integrated RED/ED hybrid system.

3. Result and discussion

3.1 Basic parameters used for model simulation

Based on the modeling of the RED/ED hybrid system in this work, there are several important independent parameters in the design. First are parameters relating to the electromotive force of the system: the ratio of RED and ED stacking pairs (N_{RED}/N_{ED}), the ratio between concentration of the high-salinity solution and low-salinity solution (C_h/C_l) and the ratio of the initial concentration of the permeate solution and feed solution ($C_{p,0}/C_{f,0}$); Second are parameters relating to the resistance of the system: N_{RED}/N_{ED}, the concentration of the low-salinity solution, C_l, the

concentration of the feed solution, $C_{f,0}$ and the thickness of the channels, δ. To clarify the effects of these parameters on the performance of the RED/ED hybrid system, the values of these parameters are assumed in **Table S1**.

3.2 The process of desalination in the RED/ED system

In one typical running process of the RED/ED hybrid system (**Figure 2**), the E_{RED} is constant due to the RED unit is assumed to be a continuous operation mode. The E_{RED} is approximately 0.18 V when the concentrations of the high-salinity solution and low-salinity solution in RED are seawater (600 mM) and river water (10 mM) (**Figure 3**). For ED in batch mode, the concentration of the permeate solution increases and the concentration of the feed solution decreases, thus causing an increase of Ψ_{ED} **(Figure 3)**. The point of intersection of E_{RED} and $\Psi_{ED}(q_e)$ indicates the theoretical maximum ratio of desalination. q_e is calculated based on **Eq. (7)** and it depends on the value of $C_{p,0}/C_{f,0}$, C_h/C_l and N_{RED}/N_{ED}. q_e increases with $C_{p,0}/C_{f,0}$ and decreases with C_h/C_l and N_{RED}/N_{ED}.

$$q_e = (1+\frac{C_{p,0}}{C_{f,0}}) \Big/ (\frac{C_h}{C_l}^{\frac{N_{RED}}{N_{ED}}} + 1) \tag{15}$$

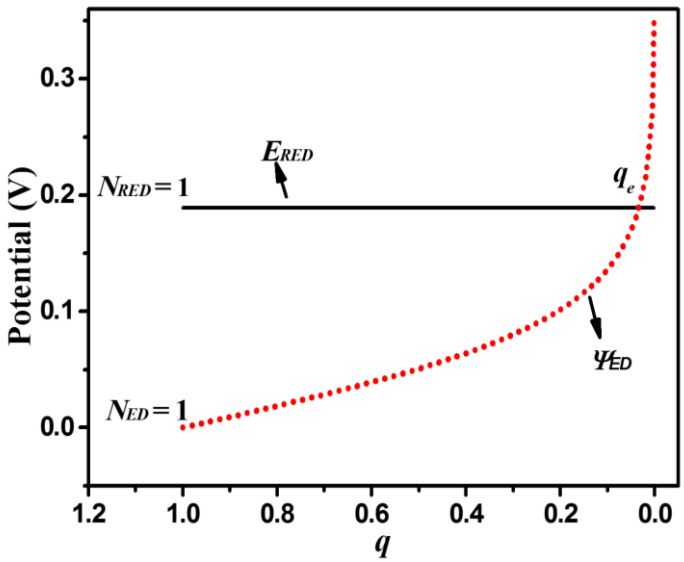

Figure 3 Calculated curves of potential difference created by RED part (E_{RED}) and ED part (Ψ_{ED}) versus q.

The process of the desalination of the feed solution is showed in **Figure 4**. The normalized area resistance ($\frac{R_{tot,q}}{N_{ED} / A_m}$) shows no obvious variation in a relatively wide range ($1 > q > 0.05$, ~ 0.022 Ω•m^2), then suddenly increases to 0.155 Ω m^2 at the end of the desalination process. When $q > 0.05$, the concentration of the feed solution is more than 30 mM, and the influence of the feed solution on the whole system resistance is insignificant, whereas when q is lower than 0.05 that is, when $C_{f,t} < 30$ mM the feed solution shows a notably effect on the whole resistance of the system, resulting in a dramatically increasing resistance from 0.022 to 0.155 Ω m^2. High resistance at the end of the desalination process was also observed in most ED systems [2].

With ongoing desalination, the net potential difference (E_{RED}-Ψ_{ED}) decreases resulting from the increased Ψ_{ED}. Both the net potential difference and the whole resistance synergistically determine the current density of the loop and the desalination time. It was found that the current density first linearly changes from 16.8 to12.1 A•m^{-2}, then sharply decreases to nearly zero. The normalized time changes following an opposite trend, that is, it linearly increases from 0 to 1.91 h•m^2/mol when q is in the range of 1 from 0.05, then sharply increases to infinity. A large amount of time will be consumed by the end of the desalination process since the high resistance results in high energy consumption and low current efficiency [25]. The time curve of desalination also indicates that the percentage of desalination in RED/ED is theoretically more than 90%.

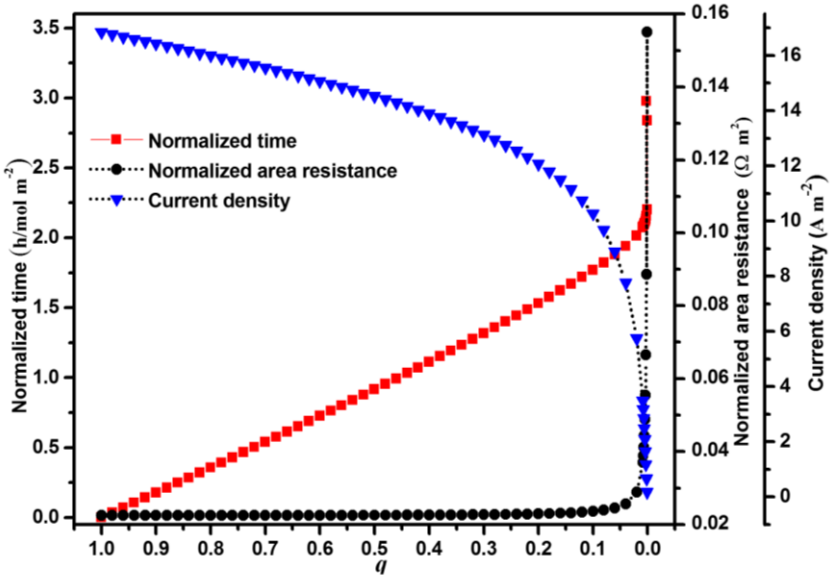

Figure 4 Calculated curves of normalized time, area resistance and current density versus degree of desalination q. Other conditions: δ = 0.5 mm, N_{RED}/N_{ED} = 2, C_h/C_l = 60, $C_{p,0}/C_{f,0}$ = 1, C_l = 10 mM, $C_{f,0}$ = 600 mM.

3.3 Effects of the design parameters on the performance of RED/ED system

In a normal case, increased electromotive force-related parameters (N_{RED}/N_{ED}, C_h/C_l, $C_{p,0}/C_{f,0}$) and decreased resistance related parameters (N_{RED}/N_{ED}, C_l, $C_{f,0}$ and δ) will accelerate the desalination process in RED/ED systems. Nevertheless, the influences of C_l and N_{RED}/N_{ED} on the desalination process are competitive. Therefore, it is necessary to discuss the effects of these parameters on the performance of the system to find a better adaptation of RED/ED.

3.3.1 Effects of C_l on the desalination process

Figure 5a shows several combinations of RED streams, in which the high-salinity water is always seawater (600 mM), whereas a wide range of concentrations (1-100 mM) are used for the low salinity water. It is found that the desalination time decreases first (C_h/C_l changes from 600 to 20) and then increases (C_h/C_l changes from 20 to 6) with increasing C_l. The decreased electromotive force and reduced internal resistance competitively affect the desalination process. When C_l is less than 30 mM,

the influence on resistance from C_l is larger than that on the electromotive force from C_h/C_l in desalination. Therefore, increasing C_l from 1 to 30 mM will greatly lower the system resistance and accelerate the desalination process. When C_l changes from 30 to 100, the influence of the decreased C_h/C_l (from 20 to 6) on the electroforce of the system play a prominent role, leading to a lower desalination rate. Aiming at learning the effects of C_l on desalination in more detail, the initial slopes are plotted with C_l from 1 to 200 mM (**Figure S2**). The smaller slope indicates a lesser time cost and a higher rate of desalination. The minimal initial slope (using the absolute value, which is the same as the following slope) is 0.64 h•m^2/mol, corresponding to C_l values in the range of 10-20 mM (**Figure S2**). Analogous results were also shown in a standalone RED system and the maximum power density occurred at C_l over 10-20 mM [23].

Similar results are observed when the high-salinity water is brine (5000 mM) (**Figure 5b**). The optimal initial slope is 0.38 h•m^2/mol, which is 59% smaller than that from using seawater as high-salinity water. The optimal condition C_l occurs at 20-30 mM (**Figure S2**). No matter whether seawater or brine water is used as the high-salinity water in the RED unit, the optimal concentration of the low-salinity water C_l is approximately 20 mM, indicating that river water (approximately 17 mM) can be an excellent candidate for the low-salinity water in the RED unit. However, the optimal C_l for the RED electroforce could depend on the stack configuration and operation conditions. For example, an increased number of membrane pairs would favor a higher C_l concentration, while a decreased channel thickness would favor a lower C_l concentration [26, 27]. Therefore, wastewater (5-100 mM) and diluted seawater also have potential to be used as the low-salinity stream [28, 29].

3.3.2 Effects of N_{RED}/N_{ED} and $C_{p,0}/C_{f,0}$ on the desalination process

Figure 5c shows the effects of N_{RED}/N_{ED} on the RED/ED desalination process. It

was found that the initial slope greatly decreases from 2.27 to 1.72 h•m^2/mol as N_{RED}/N_{ED} increases from 1 to 4, then tends toward a saturation value of 1.67 h•m^2/mol as N_{RED}/N_{ED} increases from 4 to 8 (**Figure S3**). A higher N_{RED}/N_{ED} means a higher net potential energy (E_{RED}-$\Psi_{ED,q}$), resulting in faster desalination. In this model, a value of N_{RED}/N_{ED} of more than 4 should be suitable for a high performance of the RED/ED system. However, the cost of membranes, spacers, pump energy, etc., will correspondingly increase with N_{RED}/N_{ED}, Therefore, a more systematic model including efficiency and economy is required to investigate the optimized value of N_{RED}/N_{ED} in future work.

Figure 5d shows the effects of the ratio of the concentration of the permeate solution to that of the feed solution ($C_{p,0}/C_{f,0}$) on the performance of the RED/ED hybrid system. The initial slope decreases as $C_{p,0}/C_{f,0}$ increase from 1 to 10 due to the lowered driving force (E_{RED}-$\Psi_{ED,q}$). In a normal case, seawater used as both the permeate solution and the feed solution is suitable for RED/ED desalination.

3.3.3 Effects of the thickness of the channels and the feed solution on the desalination process

The effects of fluid channels, δ, on the performance of the RED/ED system are shown in **Figure 5e.** The initial slope of the time curve is linearly enhanced from 0.67 to 1.80 h•m^2/mol as δ increases from 0.1 to 1.0 mm (**Figure S4**). Thin compartments will reduce the intermembrane distances, lower the resistance and consequently accelerate salt removal. However, more energy will be used in pumping the streams into the device, causing extra energy consumption. In a standalone RED, the net power density output was reduced from 1.2 to 0.75 W/m^2 when the intermembrane distance was lowered from 0.1 mm to 0.06 mm [27]. Therefore, the design of an efficient and low-energy RED/ED system should compromise between the pump

energy consumption and the rate of desalination. Varying the concentration of feed solution (100-1000 mM) has little influence on the performance of the RED/ED system **(Figure 5f**). Since the molar mass of the feed solution is normalized, the effect of the feed solution is mainly from its resistance. However, when $C_{f,0}$ is 100 mM, the desalination process slows down after q becomes less than 0.6, corresponding to $C_{f,0}$ < 60 mM. The resistance of the feed solution starts to play a noticeable role in the performance of the system. Therefore, the RED/ED system is not suitable for deep desalination.

Based on the above discussion, it is important to remark that the following information is gained from this model: First, when seawater or brine is used as the high salinity water, C_l value of 10-20 mM or 20-30 mM are preferred, which is similar to that for the standalone RED of former works [23, 26]. Second, the enhanced N_{RED}/N_{ED} and the decreased thickness of the channels, δ, greatly accelerate the RED/ED desalination process. Third, seawater is suitably used both as the feed and as the permeate solution. When the concentration of the feed water is less than 60 mM, it starts to exert a notable influence on the performance of the RED/ED. Therefore, the RED/ED system is more suitable for the pre-desalination of seawater.

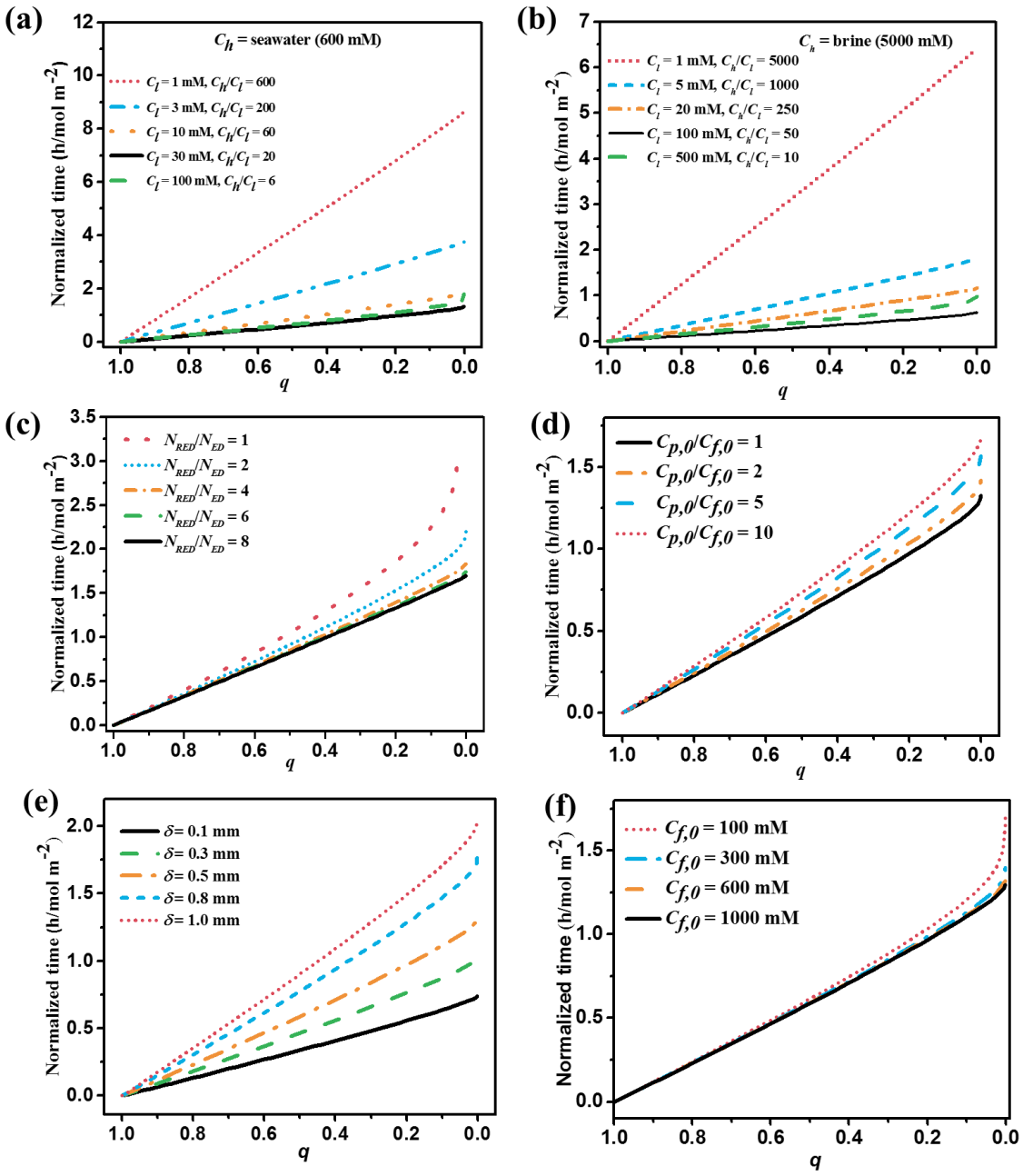

Figure 5 (a, b) Effects of C_l on the desalination process when the C_h is seawater (**a**) or brine (**b**)**.** Conditions**:** δ = 0.5 mm, $C_{p,0}/C_{f,0}$ = 1, $C_{f,0}$ = 600 mM. N_{RED}/N_{ED} = 4. **(c)** Effects of N_{RED}/N_{ED} on the desalination process. δ = 0.5 mm, $C_{p,0}/C_{f,0}$ = 1, $C_{f,0}$ = 600 mM, C_h/C_l = 60, C_l = 10 mM. (**d**) Effects of $C_{p,0}/C_{f,0}$ on the desalination process. δ = 0.5 mm, N_{RED}/N_{ED} = 4, $C_{f,0}$ = 600 mM, C_h/C_l = 60, C_l = 10 mM. **(e)** Effects of thickness of channels on the desalination process. Conditions: $C_{p,0}/C_{f,0}$ = 1, C_h/C_l = 60, C_l = 10 mM, N_{RED}/N_{ED} = 4, $C_{f,0}$ = 600 mM. **(f)** Effects of $C_{f,0}$ on the desalination process. Conditions: $C_{p,0}/C_{f,0}$ = 1, C_h/C_l = 60, C_l = 10 mM, δ = 0.5 mm, N_{RED}/N_{ED} = 4.

3.4 Model evaluation

To verify this model, experimental data on RED (*Case I* and *Case II*), ED (*Case III*) or RED/ED (*Case IV* and *Case V*) from published works were used to assess the model. The main parameters of *Case I-V* are shown in **Table S2.**

3.4.1 RED model evaluation using the experimental data of *Case I* and *Case II*

The RED unit is the power generation unit of the hybrid system. The electric potential, E_{RED}, and the resistance, R_{RED}, are the two important indexes for evaluation of the RED unit. **Figure 6a** shows that the E_{RED} decreases from 1.28 V to 0.88 V as the concentration of low-salinity of solution increases from 0.002 M to 0.08 M. However, when the high-salinity solution (e.g. brine) is used as the stream, correction of the permselectivity should be performed in IEM, shown in **Figure 6b**. The high-salinity solution will deteriorate the permselectivity of the IEMs. The value of the correction coefficient depends on the properties of the membranes. For example, the permselectivity of the membrane (Selemion) decreased from 0.9 to 0.85 when the concentration of the high salinity solution increased from 0.6 M to 2 M (**Figure 6b**), while that of Fujifilm changed from 0.8 to 0.4 when brine was used [14, 23]. In addition, thinner IEMs (20 μm) show better permselectivity (~0.6) than do thicker IRMs (120 μm, ~0.4-0.5) [14, 30]. When C_l is higher than 0.02 M, the value of R_{RED} in the simulated data is 0.5~1.0 Ω lower than the experimental data (**Figure 6b, Figure S5**). This difference results from omitting the resistance of the electrode system and high salinity solution. This difference will be negligible with a large number of cells stacked in the RED unit. The good accordance between the experimental data and the simulated data indicates that the mathematical model developed herein effectively captures the RED process, as shown in **Figure 6a, 6b.**

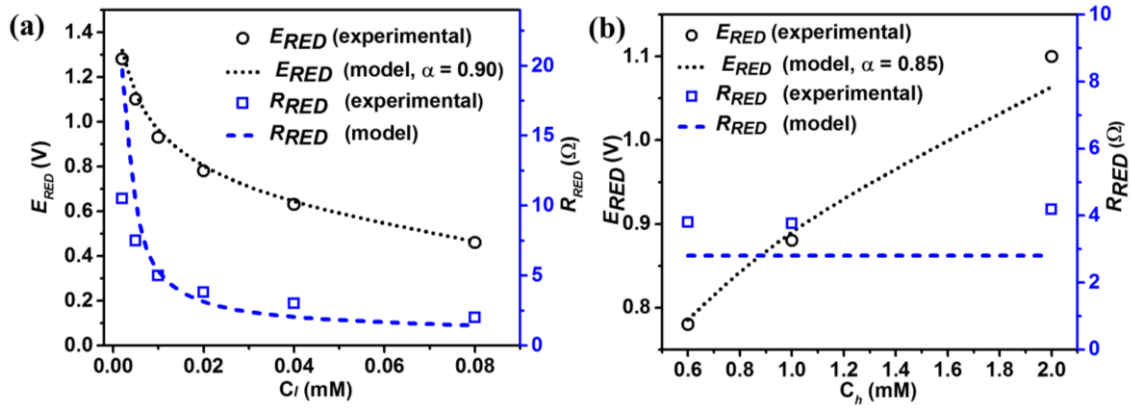

Figure 6 Model evaluation with the experimental data of *Case I* (**a, b**).

3.4.2 ED model evaluation using the experimental data of *Case III*

The kinetic profiles of the desalination process were used as for evaluation of the ED model. **Figure 7** shows that the rate of desalination decreased when the applied voltage changed from 1.00 V to 0.50 V per cell pair. At each voltage applied, the rate of desalination slows with time due to the high resistance generated by the feed solution. All the three trends were reasonably captured by the model, which supports the predictive capability of this developed model in the ED unit.

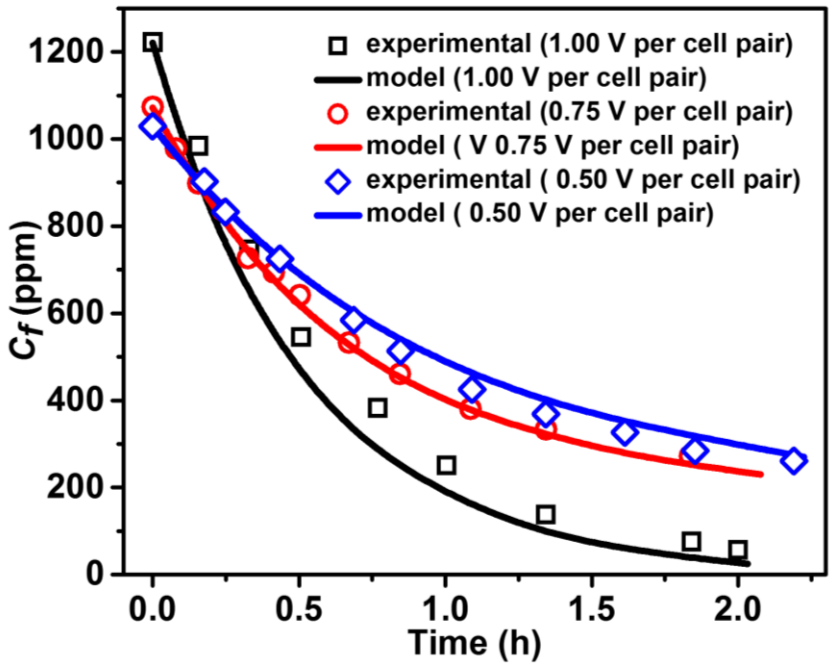

Figure 7 Model evaluation with the experimental data of *Case III*.

3.4.3 RED/ED model evaluation using the experimental data of *Case IV*

The experimental data of the RED/ED hybrid system (*Case IV*) suggested that the best value of N_{RED}/N_{ED} is 2.6, considering the function and cost of the system [17]. In our work, a value of N_{RED}/N_{ED} higher than 4 is preferred without regard to the cost of the system. However, values of 2-4 of N_{RED}/N_{ED} are suggested as the better option in consideration of cost. A more systematical model including cost calculation is required to obtain the precise value of N_{RED}/N_{ED}. **Table 1** shows a comparison of experimental data with modeling data from internal-integrated RED/ED. The values of E_{RED} from the developed model are 28.1% higher than the obtained data from *case IV*, resulting in a higher current density (26.8%) and a faster rate of desalination (23.0%). The bias of E_{RED} is mainly due to the low velocity (0.471 cm/s) of the streams. It was found that the E_{RED} increased by 10-15% after the velocity increased from 0.5 cm/s to 1.0 cm/s [15]. In addition, the salt leakage and permselectivity of the IEMs also cause the bias of the experimental data relative to the modeling data. Thereby, correction coefficient (~1.3) for better describing the desalination process should be introduced into the normalized time.

Moreover, it is interesting to find that the correction coefficient is 2.7 when this model is used to simulate the external-integrated RED+ED system, as shown in **Figure 8**. This indicates that the desalination rate of the internal-integrated mode is ~2 times higher than that of the external-integrated mode. The lower desalination rate of the external-integrated mode may result from the energy conversion in two-electrode systems. The salinity gradient energy harvested from RED must first be converted to electrical energy and can drive the ED unit to desalt again via the electrode system. Therefore, the desalination in an internal-integrated RED/ED system shows a higher energy efficiency than that of RED+ED systems. **Figure 8** shows that this model well

matches well the trends of desalination from RED+ED after correction, again proving the predictive power of this model.

Table 1 Comparison of experimental data of *Case IV* of and modelling data.

Entry	E_{RED} (V)	Current density ($A \cdot m^{-2}$)	Rate of desalination ($h/mol\ m^{-2}$)	Reference
Experimental	1.35	8.2	3.7	[17]
Modelling	1.73	10.4	2.85	This work
Bias (%)	28.1	26.8	23.0	This work

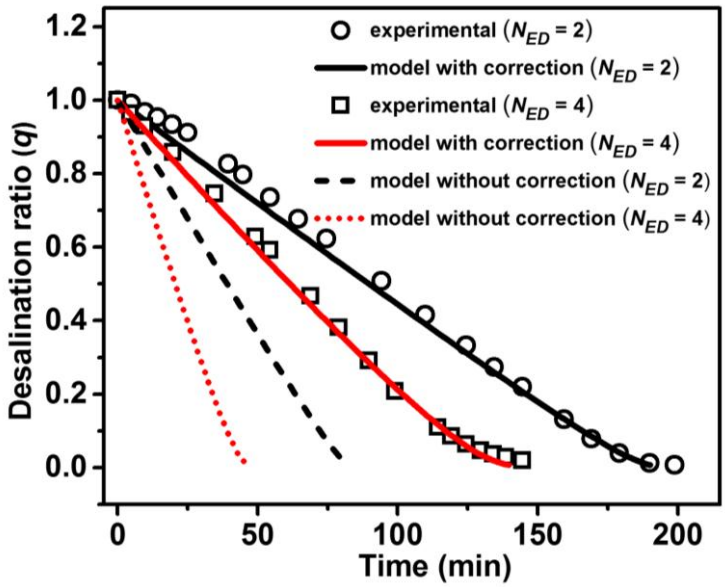

Figure 8 Model evaluation with the experimental data of *Case V* before and after correction.

3.5 Desalination comparison with literature

In this internal-integrated RED/ED hybrid system, the energy extracted from RED is wholly used for desalination in the ED unit with a capacity of desalination of 0.43-2.6 $mol/h \cdot m^2$, which is higher than that achieved by external-integrated RED+ED hybrid system (0.10-0.15 $mol/h \cdot m^2$) (**Table 2, entry 1, 2**) [15]. The ion current in RED is directly used for desalination, resulting in the higher energy conversion efficiency of the RED/ED system [15]. The energy consumed for pumping in RED/ED (0.004-0.065 kWh/m^3) is also lower than that in RED+ED (0.062-0.28 kWh/m^3). Moreover, only one electrode is required in the internal-integrated RED/ED,

suggesting a more economical design mode. This device is more suitable for a pre-desalination process rather than for deep desalination because a higher energy consumption and lower current efficiency are found at the end of the desalination process. The standalone RED has been considered as a pre-desalination device with a capacity of desalination of only 0.002-0.3 mol/h•m^2 [15, 31, 32]. Moreover, the percentage of desalination in RED is less than 50%; thus, a large amount of energy is still required for another 50% salt removal, such as the RED/RO (0.7-0.8 kWh/m^3) [32] or RED+ED systems [15]. However, through configuring the RED/ED hybrid system, the percentage of desalination could theoretically be more than 90%, which is much higher than that of a standalone RED. Therefore, it will be more energy-economic when RED/ED is coupled with other desalination technologies, such as RED/ED+RO or RED/ED+ED. The energy required in RO or ED is only used for the extra 10% salt removal, which will greatly reduce the total energy requirement. Though the capacity for desalination of the RED/ED system is still lower than that of wind/ED (6.3-11.4 mol/h•m^2) or solar/ED (0.3-7.7 mol/h•m^2), the lower investment, simpler construction and lower energy consumption still make RED/ED a valuable device for desalination (**Table 2, entry 3, 4**) [4] [7, 33].

Table 2 Capacity of desalination and energy requirement in different systems.

Entry	System	Capacity of desalination (mol/h•m^2)	Required energy (kWh/m^3)	Reference
1	RED/ED	0.43-2.6	0.004-0.065[a]	This work
2	RED+ED	0.10-0.15	0.062-0.28[a]	[15]
3	Wind/ED	6.3-11.4	2.5-4.2	[4]
4	Solar/ED	0.3-7.7	0.7-1.7	[7, 33]
5	RED	0.002-0.3	-----	[32]

[a] Energy input for pumping in RED was calculated; seawater (0.6 M) is used as the feed water, the final concentration of feed water is drinkable water (500 mg/L, 0.008 M); the flow rate in RED is 20-50 L/min.

4. Perspectives

RED is always combined with brine as RED can extract the chemical energy from brine for a higher energy output, meanwhile solving the disposal of brine [34, 35]. In the RED/ED system, a higher performance of desalination is obtained from using brine than that from using seawater as the high-salinity water, with a maximum desalination rate of 0.38 h•m^2/mol. In this model, we assumed that all four streams are independent (**Figure 9a**). However, for practical application, the brine generated from ED could be guided into the high-salinity water of RED to create a higher salinity gradient energy, accelerating the process of desalination while reducing the salinity of the brine (**Figure 9b**). Seawater in the RED unit can also be first desalted and then guided into the feed solution of the ED for further desalting, as shown in **Figure 9c**.

Previous reports mentioned that thin fluid channels would increase the pump energy and reduce nonohmic resistance in the diffusion boundary layer [36]. In this model, we assumed that the thickness of each channel is the same. In practical design, it is feasible to design a different thickness for each channel to obtain a better performance of the system. For example, thicker channels can be used for the high salinity solutions to minimize the pump energy, while thinner channels can be used for the low salinity solutions where the electrical resistance plays an important role. Thus, more detailed optimization will require the model to further incorporate the effects of channel thickness with pump energy, an aspect that requires further study in the context of RED/ED hybrid desalination.

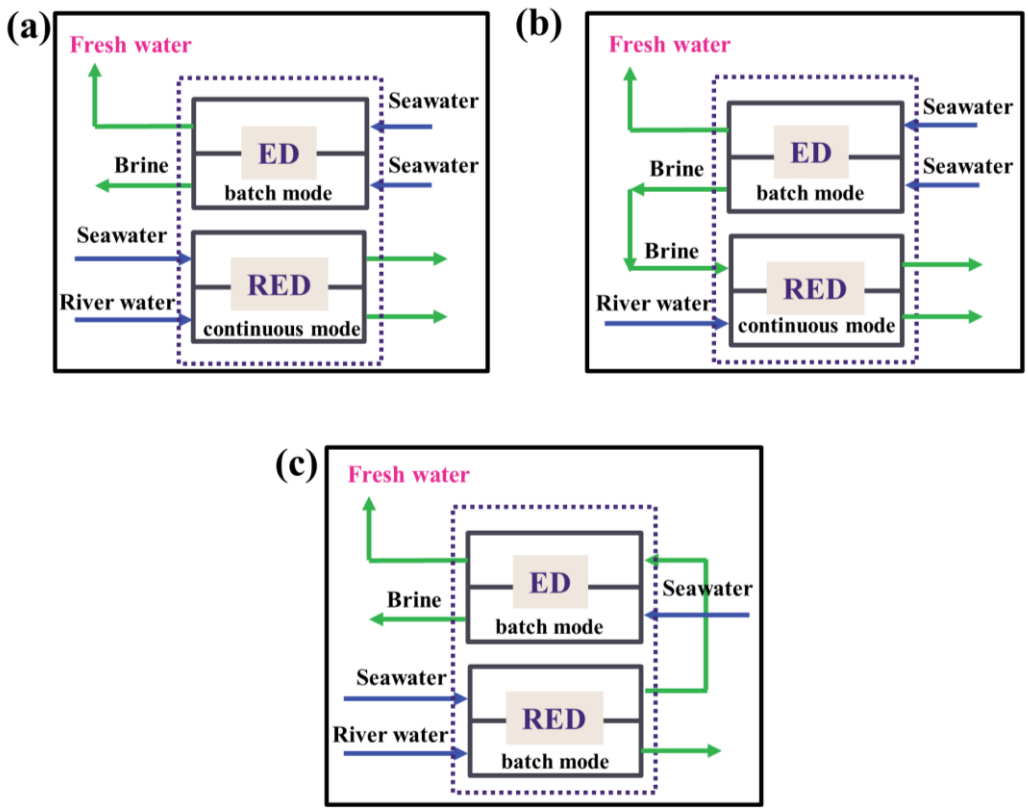

Figure 8 Different scenarios were proposed for the RED/ED system.

5. Conclusions

In this study, an analytical model of an internal-integrated RED/ED hybrid system is developed to investigate the effects of design parameters on the performance of self-sufficient desalination. The desalination capacity of RED/ED (0.43-2.6 mol/h•m^2) is much higher than that of external-integrated RED+ED system (0.1-0.15 mol/h•m^2), but the system is of simpler configuration and lower energy requirement. Although the capacity for desalination by RED/ED is lower than that of conventional sustainable energy-driven ED, e.g., solar/ED or wind/ED, the lower investment, lower energy requirement and better brine managements still make RED/ED a potential device for desalination. When seawater is used as the feed water, the percentage of desalination in RED/ED is higher than 90%. Brine/river are the optional natural streams for practical application, with a desalination rate of 0.38 h•

m^2/mol. Due to the high resistance at the end of desalination, the RED/ED system is preferred to be used in the pre-desalination process. This model is helpful in the design of RED/ED systems, and points out the development potential of RED/ED in practical applications.

Acknowledgements

This work is supported by a grant from the Research Grants Council of the Hong Kong Special Administration Region, China (C7051-17G) and National Natural Science Foundation of China (21607023).

Nomenclature

A_m	area of each membrane (m^2)
C	concentration of solution (mol/m^3)
C_{NaCl}	concentration of NaCl solution (mol/m^3)
$C_{f,0}$	initial concentration of feed solution (mol/m^3)
$C_{f,q}$	concentration of feed solution when desalination ratio is equal to q (mol/m^3)
$C_{p,q}$	concentration of permeate solution when desalination ratio is equal to q (mol/m^3)
C_l	concentration of low salinity water (mol/m^3)
C_h	concentration of high salinity water (mol/m^3)
E_{RED}	electric potential in reverse electrodialysis (V)
F	faraday constant (96,485 C/mol)
f	feed solution
f_v	obstruction factor
h	high salinity water
I	current of circuit
k	normalized parameter ($h/mol\ m^{-2}$)
l	low salinity water
N_{ED}	number of cells in electrodialysis stack
N_{RED}	number of cells in reverse electrodialysis stack
p	permeate solution
q	desalination ratio
Q_h	volumetric flow rates of high salinity solution compartment (m^3/s)
Q_l	volumetric flow rates of low salinity solution compartment (m^3/s)
Q_f	volumetric flow rates of feed solution compartment (m^3/s)
Q_p	volumetric flow rates of permeate solution compartment (m^3/s)
R	gas constant (8.314 J/mol K)
$R_{ED,q}$	resistance in electrodialysis (Ω)
R_{RED}	resistance of RED part (Ω)
$R_{tot,q}$	total resistance of RED/ED hybrid system when desalination ratio is equal to q (Ω)
$\overline{R}_{AEM}$	area resistance for the AEM ($\Omega \cdot m^2$)
$\overline{R}_{CEM}$	area resistance for the CEM ($\Omega \cdot m^2$)
$\overline{R}$	area resistance ($\Omega \cdot m^2$)
$\overline{R}_{NaCl}$	area resistance of NaCl solution ($\Omega \cdot m^2$)
V_f	volume of feed solution (V)
T	absolute temperature (K)
Z	valence
+	cation

-	anion ion
Δp_h	pressure drops along high salinity solution compartment (Pa)
Δp_l	pressure drops along low salinity solution compartment (Pa)
Δp_f	pressure drops along feed solution compartment (Pa)
Δp_p	pressure drops along permeate solution compartment (Pa)

Greek symbols

α_{CEM}	permselectivity of the cation exchange membrane
α_{AEM}	permselectivity of the anion exchange membrane
Λ_m	equivalent conductivity of solution ($m^2 \cdot mol^{-1} \cdot \Omega^{-1}$)
$\Psi_{ED,q}$	potential different in electrodialysis when desalination ratio is equal to q (V)
$\gamma_{\pm}$	mean activity coefficients
δ	thickness of the fluid channels (m)
η	current efficiency

Abbreviations

AEM	anion exchange membrane
CEM	cation exchange membrane
ED	electrodialysis
RED	reverse electrodialysis
RED/ED	internal-integrated reverse electrodialysis and electrodialysis
RED+ED	external-integrated reverse electrodialysis and electrodialysis
RO	Reverse osmosis
IEM	Ion exchange membrane

References

[1] J.R. Werber, C.O. Osuji, M. Elimelech, Materials for next-generation desalination and water purification membranes, Nat. Rev. Mater., 1 (2016) 16018.

[2] F. Zhang, M. Chen, Y. Zhang, R.J. Zeng, Microbial desalination cells with ion exchange resin packed to enhance desalination at low salt concentration, J. Membrane Sci., 417 (2012) 28-33.

[3] A. Ali, R.A. Tufa, F. Macedonio, E. Curcio, E. Drioli, Membrane technology in renewable-energy-driven desalination, Renew. Sust. Energ. Rev., 81 (2018) 1-21.

[4] P. Malek, J.M. Ortiz, H.M.A. Schulte-Herbrüggen, Decentralized desalination of brackish water using an electrodialysis system directly powered by wind energy, Desalination, 377 (2016) 54-64.

[5] A. Al-Karaghouli, L.L. Kazmerski, Energy consumption and water production cost of conventional and renewable-energy-powered desalination processes, Renew. Sust. Energ. Rev., 24 (2013) 343-356.

[6] K.M. Chehayeb, H.L.V. John, Entropy generation analysis of electrodialysis, Desalination, 413 (2017) 184-198.

[7] F. Cirez, J. Uche, A.A. Bayod, A. Martinez, Batch ED fed by a PV unit: a reliable, flexible, and sustainable integration, Desalin. Water. Treat., 51 (2013) 673-685.

[8] R. Long, B. Li, Z. Liu, W. Liu, Reverse electrodialysis: Modelling and performance analysis based on multi-objective optimization, Energy, 151 (2018) 1-10.

[9] A.H. Avci, R.A. Tufa, E. Fontananova, G. Di Profio, E. Curcio, Reverse Electrodialysis for energy production from natural river water and seawater, Energy, 165 (2018) 512-521.

[10] Y. Mei, C.Y.Y. Tang, Recent developments and future perspectives of reverse electrodialysis technology: A review, Desalination, 425 (2018) 156-174.

[11] R.A. Tufa, S. Pawlowski, J. Veerman, K. Bouzek, E. Fontananova, G.D. Profio, S. Velizarov, J.G. Crespo, K. Nijmeijer, E. Curcio, Progress and prospects in reverse electrodialysis for salinity gradient energy conversion and storage, Appl. Energ., 225 (2018) 290-331.

[12] M. Bevacqua, A. Tamburini, M. Papapetrou, A. Cipollina, G. Micale, A. Piacentino, Reverse electrodialysis with NH_4HCO_3-water systems for heat-to-power conversion, Energy, 137 (2017) 1293-1307.

[13] K. Kwon, J. Han, B.H. Park, Y. Shin, D. Kim, Brine recovery using reverse electrodialysis in membrane-based desalination processes, Desalination, 362 (2015) 1-10.

[14] M. Tedesco, E. Brauns, A. Cipollina, G. Micale, P. Modica, G. Russo, J. Helsen, Reverse electrodialysis with saline waters and concentrated brines: A laboratory investigation towards technology scale-up, J. Membr. Sci., 492 (2015) 9-20.

[15] Q. Wang, X. Gao, Y. Zhang, Z. He, Z. Ji, X. Wang, C. Gao, Hybrid RED/ED system: Simultaneous osmotic energy recovery and desalination of high-salinity wastewater, Desalination, 405 (2017) 59-67.

[16] F.B. Luo, Y.M. Wang, C.X. Jiang, B. Wu, H.Y. Feng, T.W. Xu, A power free electrodialysis (PFED) for desalination, Desalination, 404 (2017) 138-146.

[17] Q. Chen, Y.Y. Liu, C. Xue, Y.L. Yang, W.M. Zhang, Energy self-sufficient desalination stack as a potential fresh water supply on small islands, Desalination, 359 (2015) 52-58.

[18] P.A. Sosa-Fernandez, J.W. Post, H. Bruning, F.A.M. Leermakers, H.H.M. Rijnaarts, Electrodialysis-based desalination and reuse of sea and brackish polymer-flooding produced water, Desalination, 447 (2018) 120-132.

[19] E.Y. Choi, J.H. Choi, S.H. Moon, An electrodialysis model for determination of

the optimal current density, Desalination, 153 (2003) 399-404.

[20] F. Galvanin, R. Marchesini, M. Barolo, F. Bezzo, M. Fidaleo, Optimal design of experiments for parameter identification in electrodialysis models, Chem. Eng. Res. Des., 105 (2016) 107-119.

[21] M. Tedesco, A. Cipollina, A. Tamburini, W. van Baak, G. Micale, Modelling the Reverse ElectroDialysis process with seawater and concentrated brines, Desalin. Water Treat., 49 (2012) 404-424.

[22] E.G. Lee, S.H. Moon, Y.K. Chang, I.K. Yoo, H.N. Chang, Lactic acid recovery using two-stage electrodialysis and its modelling, J. Membrane Sci., 145 (1998) 53-66.

[23] Y. Mei, C.Y. Tang, Co-locating reverse electrodialysis with reverse osmosis desalination: Synergies and implications, J. Membrane Sci., 539 (2017) 305-312.

[24] X.P. Zhu, W.H. He, B.E. Logan, Reducing pumping energy by using different flow rates of high and low concentration solutions in reverse electrodialysis cells, J. Membrane Sci., 486 (2015) 215-221.

[25] T. Xu, C. Huang, Electrodialysis-based separation technologies: A critical review, AIChE J., 54 (2008) 3147-3159.

[26] J. Veerman, M. Saakes, S.J. Metz, G.J. Harmsen, Reverse electrodialysis: Performance of a stack with 50 cells on the mixing of sea and river water, J. Membrane Sci., 327 (2009) 136-144.

[27] D.A. Vermaas, M. Saakes, K. Nijmeijer, Doubled Power Density from Salinity Gradients at Reduced Intermembrane Distance, Environ. Sci. Technol., 45 (2011) 7089-7095.

[28] A. Daniilidis, D.A. Vermaas, R. Herber, K. Nijmeijer, Experimentally obtainable energy from mixing river water, seawater or brines with reverse electrodialysis,

Renew. Energ., 64 (2014) 123-131.

[29] M. Tedesco, A. Cipollina, A. Tamburini, I.D.L. Bogle, G. Micale, A simulation tool for analysis and design of reverse electrodialysis using concentrated brines, Chem. Eng. Res. Des., 93 (2015) 441-456.

[30] M. Tedesco, H.V.M. Hamelers, P.M. Biesheuvel, Nernst-Planck transport theory for (reverse) electrodialysis: III. Optimal membrane thickness for enhanced process performance, J. Membrane Sci., 565 (2018) 480-487.

[31] K. Loganathan, P. Chelme-Ayala, M.G. El-Din, Treatment of basal water using a hybrid electrodialysis reversal-reverse osmosis system combined with a low-temperature crystallizer for near-zero liquid discharge, Desalination, 363 (2015) 92-98.

[32] W.Y. Li, W.B. Krantz, E.R. Cornelissen, J.W. Post, A.R.D. Verliefde, C.Y.Y. Tang, A novel hybrid process of reverse electrodialysis and reverse osmosis for low energy seawater desalination and brine management, Appl. Energy, 104 (2013) 592-602.

[33] J.M. Ortiz, E. Exposito, F. Gallud, V. Garcia-Garcia, V. Montiel, A. Aldaz, Desalination of underground brackish waters using an electrodialysis system powered directly by photovoltaic energy, Sol. Energ. Mat. Sol. C., 92 (2008) 1677-1688.

[34] M. Tedesco, C. Scalici, D. Vaccari, A. Cipollina, A. Tamburini, G. Micale, Performance of the first reverse electrodialysis pilot plant for power production from saline waters and concentrated brines, J. Membrane Sci., 500 (2016) 33-45.

[35] M. Tedesco, A. Cipollina, A. Tamburini, G. Micale, Towards 1 kW power production in a reverse electrodialysis pilot plant with saline waters and concentrated brines, J. Membrane Sci., 522 (2017) 226-236.

[36] J. Veerman, M. Saakes, S.J. Metz, G.J. Harmsen, Reverse electrodialysis: A validated process model for design and optimization, Chem. Eng. J., 166 (2011)

256-268.